A&A manuscript no.
(will be inserted by hand later)

Your thesaurus codes are:
03(09.13.2, 11.04.2, 11.06.1, 11.09.1 NGC 3077, 11.09.4, 13.19.3)

ASTRONOMY AND ASTROPHYSICS

Extensive molecular gas in the tidal arms near NGC 3077 – Birth of a dwarf galaxy?

Andreas Heithausen[1] **and Fabian Walter**[2]

[1] Radioastronomisches Institut der Universität Bonn, Auf dem Hügel 71, D-53121 Bonn, Germany, E-mail: heith@astro.uni-bonn.de

[2] California Institute of Technology, Astronomy Department 105-24, Pasadena, CA 91125, U.S.A., Email: fw@astro.caltech.edu

Received 28 April 2000, Accepted 21 June 2000

Abstract. Using the IRAM 30 m radio telescope we have mapped the tidal arm feature south–east of NGC 3077 where we recently detected molecular gas in the CO (J=1→0) and (2→1) transitions. We find that the molecular gas is much more extended than previously thought (several kpc). The CO emission can be separated into at least 3 distinct complexes with equivalent radii between 250 pc and 700 pc and all well confined over a narrow range in velocity – the newly detected complexes therefore range among the largest molecular complexes in the local universe. For one complex we have also obtained a CO (3→2) spectrum using the KOSMA 3 m radio telescope; utilizing an LVG model we find that the kinetic temperature for this complex must be about 10 K, and the H_2 volume density between 600 and 10000 cm^{-3}. Mass estimates based on virialization yield a total mass for the complexes of order $2 - 4 \times 10^7\,M_\odot$, i.e. more than the estimated molecular mass within NGC 3077 itself. This implies that interactions between galaxies can efficiently remove heavy elements and molecules from a galaxy and enrich the intergalactic medium. A comparison of the distribution of HI and CO shows no clear correlation. However, CO is only found in regions where the HI column density exceeds $1.1 \times 10^{21}\,cm^{-2}$. HI masses for the molecular complexes mapped are of the same order as the corresponding molecular masses. Because the intergalactic pressure is most likely too low to confine the complexes we conclude that they are gravitationally bound. Since the tidal arm with its molecular complexes has all the ingredients to form stars in the future, we are thus presumably witnessing the birth of a dwarf galaxy. This process could be important for the formation of dwarf galaxies especially at larger look–back times in the universe where galaxy interactions may have been more frequent.

Send offprint requests to: A. Heithausen

Key words: Galaxies: individual (NGC3077) - Galaxies: formation - Galaxies: Dwarf - Galaxies: ISM - ISM: molecules - Radio lines: ISM

1. Introduction

Over the last decades it has become clear that tidal forces during close encounters of galaxies can redistribute large masses as long tails or bridges between the interacting galaxies. The idea that part of these newly formed structures could form self–gravitating entities was proposed by Zwicky (1956). Numerical simulations (e.g. Elmegreen et al. 1993; Barnes & Hernquist 1996) support this scenario.

Observationally, tidal systems are best traced by the neutral gas phase (by means of HI observations) since it is this extended component of a galaxy which is most easily disrupted by interactions. Also, much work has been done in studying the tidal arms of interacting galaxies at optical wavelengths to find regions of active star-formation ('tidal dwarfs'). Impressive examples of tidal arms with on-going star-formation are, e.g., the Antenna galaxy (NGC 4038/39, Mirabel et al. 1992) and the Superantenna system (Mirabel et al. 1991). Based on an optical study of 42 Hickson compact groups of galaxies Hunsberger et al. (1996) speculate that up to 50% of the dwarf galaxies in such compact groups might be created by tidal interaction among giant parent galaxies.

Surprisingly little is known about molecular gas in tidal arms around interacting galaxies. However, this is an important issue since molecular clouds are the places where stars are born. The distribution of molecular gas in quiescent extragalactic objects (such as tidal arms) therefore gives clues as where to expect star formation to commence in the future.

Combes et al. (1988) were the first to detect a CO cloud outside the optical body of a galaxy (NGC 4438). Another small molecular cloud in a tidally influenced environment was detected by Brouillet et al. (1992) in a torn–out spiral arm of M 81. Smith et al. (1999) discovered a molecule rich tail in Arp 215 and argue that its metal

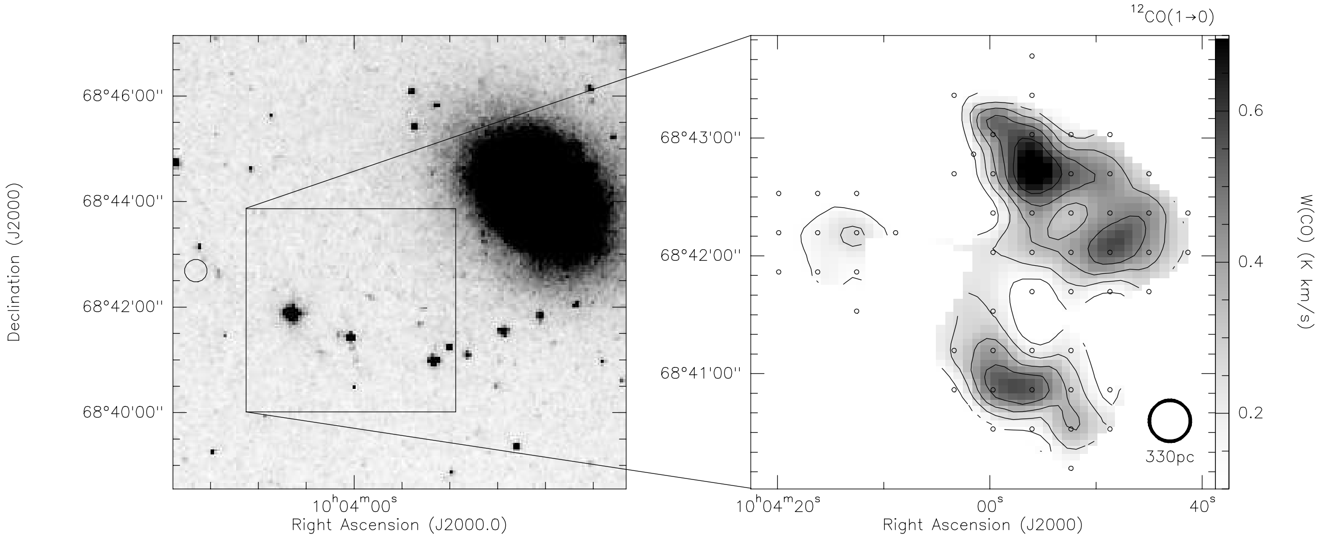

Fig. 1. Overview of the observed region. *Left:* optical image of NGC 3077 (elliptical object to the north–west) and its surrounding (taken from the digitized sky survey). For a complete optical picture of the M 81 triplet see Walter & Heithausen (1999). The box indicates the region which we mapped in CO; the open circle indicates the position towards which we searched for CO but couldn't detect any. *Right:* Blowup of our integrated CO map (J=1→0 transition). Contours are every 0.12 K km s^{-1} (2σ) starting at 0.12 K km s^{-1}. Observed positions are indicated as small circles. The beamsize is indicated in the lower right corner of the map; it corresponds to 330 pc at an adopted distance of 3.2 Mpc.

Table 1. Observed and derived parameters for molecular complexes

#	α_{J2000}	δ_{J2000}	radius (pc)	W(CO) (K km s^{-1})	v_{hel} (km s^{-1})	Δv (km s^{-1})	M_{vir} (M$_\odot$)	$M_X^{(a)}$ (M$_\odot$)	$< N$(HI) $>$ 10^{21} cm^{-2}
1	$10^h03^m56.^s0$	$68°42'41.''8$	700	0.45 ± 0.02	13.9 ± 0.3	13.5 ± 0.8	$2.4\,10^7$	$1.7\,10^7$	1.6
2	$10^h03^m56.^s0$	$68°40'51.''8$	390	0.34 ± 0.02	17.2 ± 0.4	14.7 ± 1.0	$1.6\,10^7$	$0.4\,10^7$	1.6
3	$10^h04^m16.^s5$	$68°42'11.''8$	≥ 250	0.21 ± 0.02	20.4 ± 0.4	5.2 ± 0.6	–	$\geq 0.1\,10^7$	1.4
4	$10^h04^m32.^s8$	$68°42'41.''8$	–	≤ 0.06	–	–	–	–	1.1

Remarks: Adopted distance 3.2 Mpc; $radius = \sqrt{area/\pi}$; line parameters are derived from a gaussian fit to the cloud averaged spectrum. a: $X_{\rm CO} = 8\,10^{20}$ cm^{-2} (K km s^{-1})$^{-1}$ adopted

rich gas has been driven out from the inner disk of the parent galaxy. CO–emission has also been detected in the outskirts of Cen A which can be probably attributed to its merger history (Charmandaris et al. 2000). Braine et al. (2000) described two further molecular clouds associated tidal arms of interacting galaxies, where star-formation already is taking place.

The most extended molecular complex in tidal arms of interacting galaxies was recently discovered by us near NGC 3077 (Walter & Heithausen 1999), member of the M 81 triplet. This complex is of particular interest since, although it is huge, hardly any star formation seems to be associated with it.

In this paper we present a detailed follow-up study of this complex (Walter & Heithausen 1999). Sect. 2 briefly describes our new CO observations obtained with the IRAM 30 m and the KOSMA 3 m radio telescopes. Our results are presented in Sect. 3. In Sect. 4.1 we analyze the excitation condition of the CO gas using our multi–transition observations and a simple LVG–model to match the observed line ratios. Masses for the molecular complexes are estimated in Sect. 4.2. A critical parameter for molecular gas is the shielding column density against the destroying UV radiation; we analyze the relation between HI and CO in the tidal arms in Sect. 4.3. The origin and future of the complexes are discussed in Sect. 5. We summarize our results and conclusions in Sect. 6, discuss the implications for metal loss and the enrichment of the intergalactic medium (IGM) due to gravitational interactions and speculate that we may be witnessing the birth of a new dwarf galaxy.

2. Observations

The CO (J=1→0) and (2→1) transitions have been observed in July 1999 using the IRAM 30 m radio telescope. The beam sizes are 22″ at 115 GHz and 11″ at 230 GHz (corresponding to 330 pc and 165 pc at the adopted distance of NGC 3077, 3.2 Mpc). The main beam efficiencies are $\eta_{\rm mb}(115{\rm GHz}) = 0.84$ and $\eta_{\rm mb}(230{\rm GHz}) = 0.55$, respectively. Pointing accuracy was better than 5″. Spectra were obtained with a velocity resolution of 0.8 km s^{-1} at 115 GHz and 0.4 km s^{-1} using autocorrelator spectrometers. In total, we observed 57 individual positions simultaneously in both transitions with a wobbling secondary mirror; wobbler throw was $\pm 4'$ in azimuth. The spacing between individual positions is 20″ (∼ the size of the beam at 115 GHz).

In January 2000 we also obtained one CO spectrum in the ($J = 3 \rightarrow 2$) transition using the KOSMA 3 m radio telescope located at the Gornergrat near Zermatt in the Swiss Alps. This spectrum was obtained with a wobbling secondary mirror with a throw of $\pm 3'$ in azimuthal direction. We used a medium resolution acusto-optical spectrometer with a velocity resolution which finally has been degraded to 2.3 km s^{-1}. The main beam efficiency is $\eta_{\rm mb} = 0.70$, the beam size 80″ (FWHM). The final rms is 4.8mK ($T_{\rm mb}$).

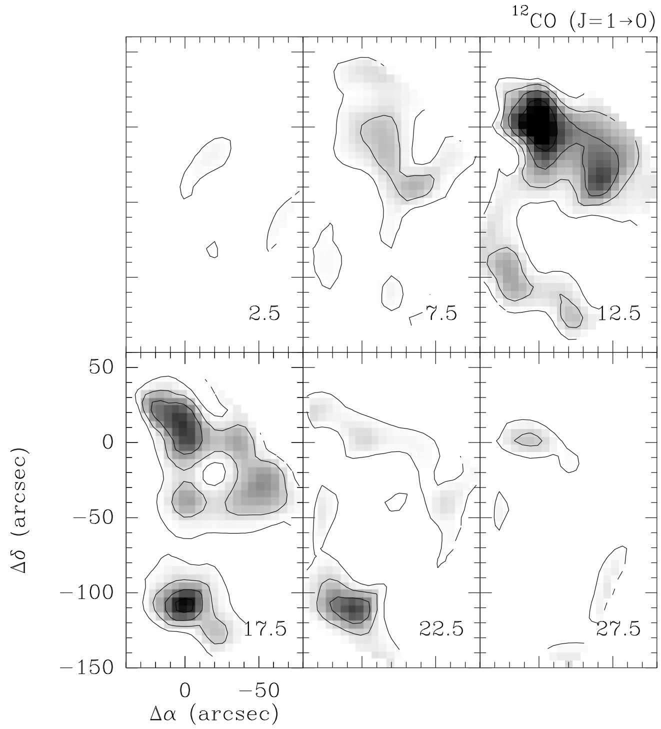

Fig. 2. Channel maps of complexes #1 and 2, averaged over 5 km s^{-1}. Center velocities of each channel are indicated in the lower right corner. Contours are every 0.012 K (2σ) starting at 0.012 K. Offsets are relative to $\alpha_{J2000} = 10^h03^m56.^s0$; $\delta_{J2000} = 68°42'41.''8$

3. Results

Fig. 1 gives an overview over our mapping results. An optical image is shown on the left (as obtained from the Digitized Sky Survey, DSS). Our CO detections (as indicated by the box and the 'X') are clearly located outside NGC 3077 (the elliptical object north–west of the centre). The area where we obtained an almost complete map in the 2 lowest CO transitions is shown in Fig. 1 (right). The CO emission is clearly extended over several kpc ($1'$ ∼1 kpc) and can be subdivided into at least two separate complexes. A further cloud ('X') has been detected outside the mapped area. This area has only partly been mapped by us as yet and an average spectrum is presented in Fig. 3.

Table 1 summarizes some observed and derived parameters for the three detected complexes. It also list a fourth position in the direction of a 'Garland' object (Karachentsev et al. 1985a) where we could not detect CO (marked as a open circle in Fig. 1, left). In Table 1 the integrated CO ($J = 1 \rightarrow 0$) line intensity, W(CO), the center velocity, $v_{\rm hel}$, and the full width at half maximum of the lines, Δv are derived from spectra averaged over the area with significant line emission of the single complexes. The radius is an equivalent radius of a circle surrounding the same area as where CO emission was detected ($radius = \sqrt{area/\pi}$).

The velocity structure of complexes #1 and #2 is visible in the channel maps displayed in Fig. 2. Cloud #1 is extended from the south–west to north–east. Complex #2 is the southern more compact object. It shows evidence for further substructure. We expect these complexes to break up in more little clouds when observed at higher spatial resolution (see also the discussion in Sect. 5). Throughout the paper we discuss only properties of the whole complexes and do not subdivide them further, although especially for complex #1 there is evidence for

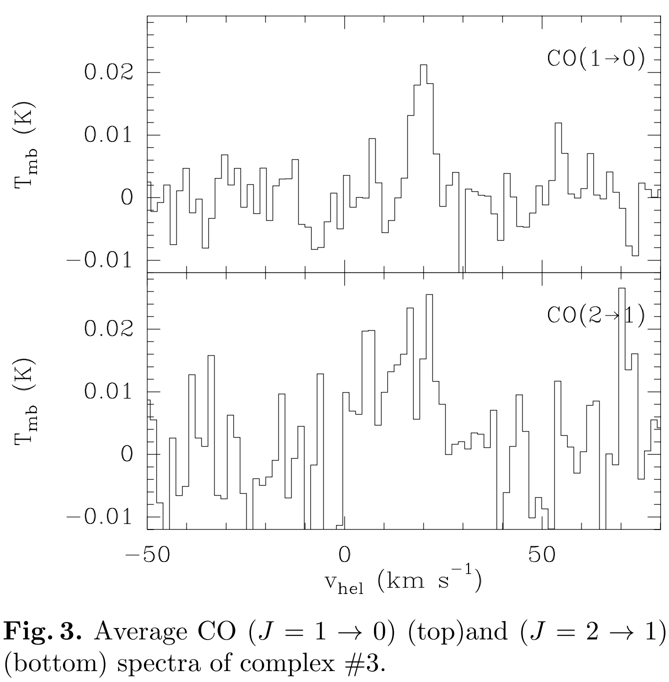

Fig. 3. Average CO ($J = 1 \rightarrow 0$) (top)and ($J = 2 \rightarrow 1$) (bottom) spectra of complex #3.

Table 2. Line parameter of CO spectra of complex #1

Transition	T_{mb} (mK)	rms (mK)	v_{hel} ($\mathrm{km\,s^{-1}}$)	Δv ($\mathrm{km\,s^{-1}}$)
$(1 \rightarrow 0)$	29	2	13.9 ± 0.3	13.4 ± 0.7
$(2 \rightarrow 1)$	17	2	11.4 ± 0.7	15.0 ± 1.6
$(3 \rightarrow 2)$	–	4.8	–	–

Remarks: The (1→0) and (2→1) spectra have been convolved to an angular resolution of 80″, the size of the KOSMA beam at 345 GHz.

Table 3. Line parameters of CO spectra of complex #2

Transition	T_{mb} (mK)	rms (mK)	v_{hel} ($\mathrm{km\,s^{-1}}$)	Δv ($\mathrm{km\,s^{-1}}$)
Center Position				
$(1 \rightarrow 0)$	63	8	19.2 ± 0.4	8.7 ± 0.9
$(2 \rightarrow 1)$	102	18	20.0 ± 0.7	10.7 ± 1.5
Average of surrounding Positions				
$(1 \rightarrow 0)$	18	3	16.6 ± 0.6	16.7 ± 1.4
$(2 \rightarrow 1)$	11	4	13.9 ± 2.2	19.7 ± 4.6

substructure in both the channel maps (Fig. 2) and in the integrated map (Fig. 1).

In order to constrain the excitation conditions of the more extended, northern complex, we have observed it with the KOSMA 3 m radio telescope in the CO (3→2) transition. The spectrum is shown in Fig. 4 together with the (1→0) and (2→1) transitions convolved to the same angular resolution as that of the KOSMA spectrum (80″, 1.3 kpc). The corresponding values derived from a gaussian analysis of the spectra are listed in Table 2. No CO (3→2) line emission was detected. The integrated line ratio for the lower two CO transitions is $R_{21} = W(2 \rightarrow 1)/W(1 \rightarrow 0) = 0.66$ with no significant variation throughout complex #1. The upper limit for the ratio of the (3→2) line to the (2→1) line is $R_{32} = W(3 \rightarrow 2)/W(2 \rightarrow 1) \leq 0.1$; implications on the excitation conditions are discussed in Sect. 4.1.

Towards complex #2 we find significant variation of the line ratio of the lower two CO transitions. Spectra towards the center of that complex are displayed in Fig. 5. The center position is easily detected in both the (1→0) and in the (2→1) transition, whereas in the surrounding positions the (2→1) transition is hardly detectable towards single positions. However, (2→1) emission is clearly present in the averaged spectrum. Values derived from a Gaussian analysis of the spectra for the center position and the average of the eight surrounding positions are listed in Table 3. The line ratio is $R_{21} = 2.0 \pm 0.4$ for the center position and $R_{21} = 0.7 \pm 0.2$ for the surrounding area. In Sect. 4.1 we discuss different beam filling and variation of the excitation conditions as possible causes for the variation of the line ratio.

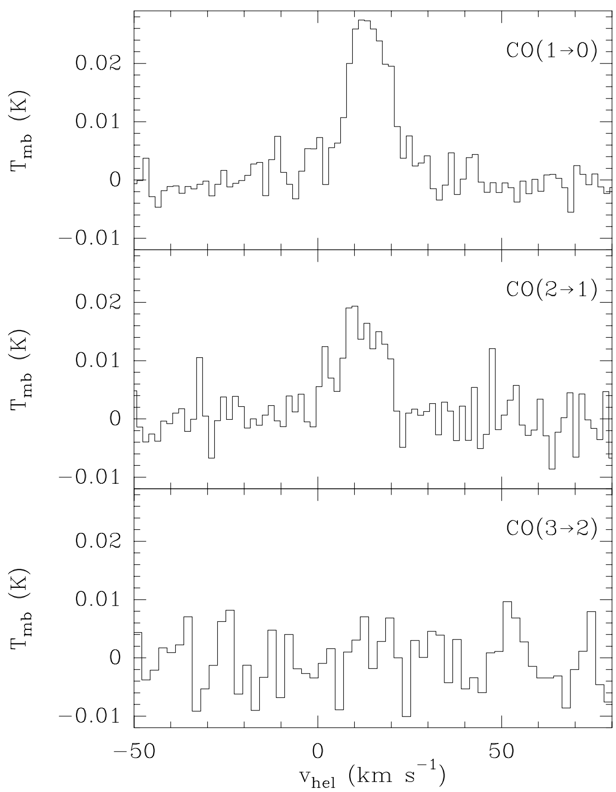

Fig. 4. CO spectra towards complex #1. The $(1 \rightarrow 0)$ and (2→1) spectra have been convolved to an angular resolution of 80″ (1.3 kpc), the size of the KOSMA beam at 345 GHz.

4. Physical parameters of the molecular gas

The molecular complex near NGC 3077 discussed here is larger than many complexes in other galaxies; e.g., the complex within NGC 3077 itself has a size (FWHM) of only 320 pc (Becker et al. 1989). The complexes near NGC 3077 are well confined over a narrow range in velocity. Cohen et al. (1988) report a full extent of the 30 Dor complex in the LMC of 2400 pc. Most Galactic molecular clouds have sizes below 60 pc (Solomon et al. 1987). The Orion A & B complexes (see Dame et al. 1987) placed at the distance of NGC 3077 would be detectable with the sensitivity of our observations, however just in one single spectrum. *The complex near NGC 3077 thus belongs to one of the largest concentrations of molecular gas in the local universe.*

4.1. Excitation conditions of the molecular gas

We will now use the ratios of the integrated line intensities to get a handle on the physical parameters. The most stringent limitations on the kinetic temperature and H_2 volume density can be derived for complex #1 for which we have observed 3 rotational transitions. In the following we apply a simple large-velocity gradient code (LVG) which adopts constant kinetic temperature and H_2 volume density throughout the cloud (see e.g. de Jong et al. 1975 for details). We calculate the line temperatures for monotonous velocity gradients of $v_{\rm grad} = 1\,{\rm km\,s^{-1}\,pc^{-1}}$ and $v_{\rm grad} = 10\,{\rm km\,s^{-1}\,pc^{-1}}$, and for CO abundances of $[{\rm CO/H_2}] = 8\times10^{-5}$ and $[{\rm CO/H_2}] = 1\times10^{-5}$. The higher CO abundance is a representative value for Milky Way clouds (e.g. Blake et al. 1987), the other was chosen to study the effects of lower metallicity.

For complex #1 the observed line ratios can only be matched if the kinetic temperature is about 10 K. The H_2 volume density should be between $600\,{\rm cm^{-3}}$, in the case of high abundance and low velocity gradient, and about $10000\,{\rm cm^{-3}}$, in the case of low abundance and high velocity gradient. The kinetic temperature is the similarly low as that for cold dark clouds in the Milky Way with no embedded massive stars, but significantly lower than that of clouds with on-going massive star-formation (e.g. Jijina et al. 1999). Note that this is a large-scale (~ 1 kpc) average value for the complex which does not exclude localized small regions which may be warmer and thus may be heated by low–level star–formation.

For complex #2 we observed only two transitions. The observed line ratio can be explained within a wide range of parameters. We can however argue that because the ratio for the outer area of that cloud is similar to that of complex #1 as a whole that also the physical conditions may be similar, i.e. low kinetic temperature and medium to high volume density. In the center of complex #2 the ratio is much higher. Part of this might be due to the different beam areas for the two transitions, 22″ for the (1→0) transition and 11″ for the (2→ 1) transition. This difference can affect the ratio by a factor of up to 4, if the observed cloud is a point source for both telescope beams.

We argue, however, that this effect only partly can account for the variation within complex #2, because it is extended in both transitions (as indicated by the presence of (2→ 1) emission in the averaged spectra surrounding the centre); in addition the line width is too wide in the (2→ 1) transition to be due to one single small molecular cloud. It is therefore more likely that indeed the kinetic temperature and/or the H_2 volume density rise in complex #2. This could be attributed to suggested on–going low–level star formation in the 'Garland' region near complex #2 (Karachentsev et al. 1985b).

4.2. Molecular cloud masses

One important yet difficult to determine physical parameter is the mass of a molecular complex. Determination of the mass is usually based on either the assumption of virialization and/or application of a $X_{\rm CO} = N({\rm H_2})/W_{\rm CO}$ conversion factor. In this section we apply both methods and discuss their pros and cons.

To estimate the $X_{\rm CO}$ factor we compare the CO luminosity for a given line width with that of a cloud with the same line width but with known molecular mass (e.g. Cohen et al. 1988). Using Fig. 2 of Cohen et al. we find that complex #1 lies within the range of values spanned by Galactic clouds, whereas complex #2 lies in the range spanned by LMC clouds. This indicates that the tidal arm clouds have CO luminosities for a given line width in between those of Milky Way and LMC clouds. The $X_{\rm CO}$ factor of the Milky Way ($\sim 2.5\times10^{20}\,{\rm cm^{-2}\,(K\ km\,s^{-1})^{-1}}$) is a factor of 6.7 lower than that of the LMC ($1.7\times10^{21}\,{\rm cm^{-2}\,(K\ km\,s^{-1})^{-1}}$, Cohen et al. 1988). Thus we use an $X_{\rm CO}$ value for the tidal arm clouds which is in between both values, $X_{\rm CO} = 8\times10^{20}\,{\rm cm^{-2}\,(K\ km\,s^{-1})^{-1}}$. This leads to molecular masses for complex #1 of $M_{X,1} = 1.7\times10^{7}\,{\rm M_\odot}$ and for complex #2 of $M_{X,2} = 0.4\times10^{7}\,{\rm M_\odot}$, (corrected for the contribution of He).

If we adopt a $1/r$ density profile through the clouds the assumption of virialization leads to masses for complex #1 of $M_{\rm vir,1} = 2.4\times10^{7}\,{\rm M_\odot}$ and for complex #2 of $M_{\rm vir,2} = 1.6\times10^{7}\,{\rm M_\odot}$. Given the uncertainties in both methods the masses for complex #1 agree well, however those for complex #2 are discrepant by a factor of 4. At this point we can only speculate which method gives the better estimate for the true molecular masses.

4.3. The relation to the HI gas

Fig. 6 shows a comparison of the distribution of the CO gas with that of atomic hydrogen. We use our high-angular resolution (13″) 21 cm map as obtained with the VLA (Walter & Heithausen 1999). It is obvious, that there is no direct correlation between the intensities of HI and CO. CO is not concentrated at the peak of the HI column density, but rather found on the outer area of the $1.5\times10^{21}\,{\rm cm^{-2}}$ contour. The average HI column density associated with complex #1 and 2 is $1.6\times10^{21}\,{\rm cm^{-2}}$, that for complex #3 is $1.4\times10^{21}\,{\rm cm^{-2}}$. At position #4 (Table 1), where no CO was found, the associated HI column density is $1.1\times10^{21}\,{\rm cm^{-2}}$.

The threshold where to find molecular gas depends on both metallicity and radiation field (e.g. Pak et al. 1998). The shielding HI column density in the tidal arms around NGC 3077 is slightly higher than values in other galaxies. In the Milky Way the H_2 threshold appears at $0.6\times10^{21}\,{\rm cm^{-2}}$ (Savage et al. 1977). CO observations of M 31 suggest a threshold of about $10^{21}\,{\rm cm^{-2}}$ (Lada et al. 1988). Young & Lo (1997) found a threshold of $0.1-0.2\times10^{21}\,{\rm cm^{-2}}$ for the dwarf elliptical galaxies NGC 185 and NGC 205; they attribute the difference to the Milky Way value and M 31 to the lower radiation field in these dwarf ellipticals. We only can speculate what causes the higher threshold in our complex. The radiation field is probably low because we do not see strong associated star forming regions.

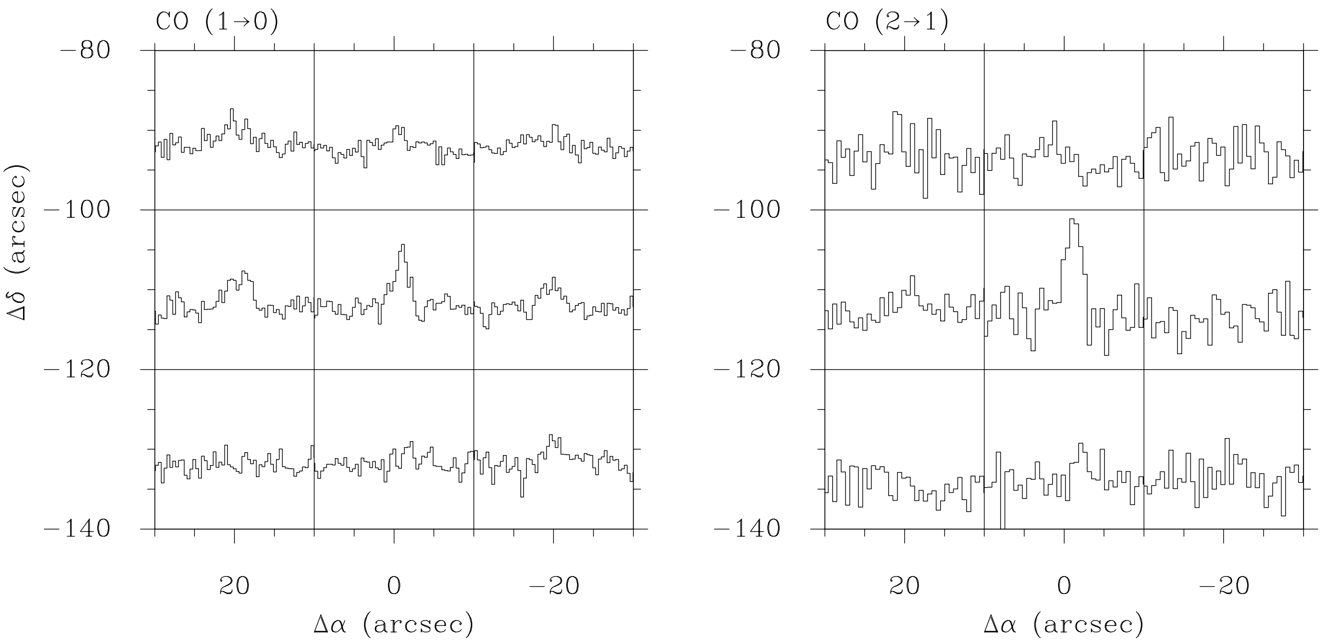

Fig. 5. CO ($J = 1 \rightarrow 0$) (left) and (2→1) (right) spectra towards complex #2. The scale for each box is $-30 \leq v_{hel} \leq 60$ km s^{-1} and $-50 \leq T_{mb} \leq 110$ mK.

The total HI mass of the tidal arm feature around NGC 3077 was found to be M(HI)=$(3-5)\times 10^8\,M_\odot$ (van der Hulst 1979, Walter & Heithausen 1999), depending on integration boundaries. If we regard only the areas where CO is detected we find an HI mass for complex #1 of about $2.7\times 10^7\,M_\odot$ and for complex #2 of about $0.8\times 10^7\,M_\odot$. These atomic masses are comparable to the molecular masses derived by our adopted $X_{\rm CO}$ factor (see Sect. 4.2).

5. Origin and future of the molecular complex

Evidently, the galaxies NGC 3077, M 81, and M 82 have undergone some violent interaction in the past. Visible signs of this interaction are the long tidal arms seen in the 21 cm line of atomic hydrogen (van der Hulst 1979, Yun et al. 1994) connecting the galaxies. According to numerical simulations the closest encounter between NGC 3077 and M 81, which presumably redistributed much of the interstellar gas in the outskirts of NGC 3077, happened some 3×10^8 years ago (Yun et al. 1993).

Now, as already discussed in Walter & Heithausen (1999) it should be stressed that it is very surprising that a huge amount of molecular gas is present at all in the tidal arm. Not only are molecular gas and hence metals present far off a galaxy but the total mass of the molecular gas in the tidal arm ($2-4\times 10^7\,M_\odot$) is possibly higher than the entire molecular mass within NGC 3077 itself ($\sim 1\times 10^7\,M_\odot$, Becker et al. 1989). It is not clear if the same ratio also holds for the total metal content in the tidal arm and in NGC 3077. In any case our finding implies that huge amounts of metal enriched material can be removed from a galaxy due to tidal interactions. This has not only important consequences for the chemical history of a single galaxy which might have undergone some interaction – interactions also seem to be able to enrich the intergalactic medium.

Regarding the molecular complex, an important question is which process condenses the molecular gas. Are the complexes pressure confined or gravitationally bound? While it is hard to imagine that a structure of kpc size is pressure confined, the intergalactic pressure is most likely too low. If we use the results from our excitation study (Sect. 4.1) the internal pressure in the molecular gas is $n\times T \geq 10^4$ cm^{-3} K. From X-ray observations with ROSAT Bi et al. (1994) found an intergalactic volume density of less than 1.5×10^{-3} cm^{-3} in the region of the tidal arm around NGC 3077. The intergalactic gas thus must have a temperature of more than 10^7 K to confine the molecular gas, which is unlikely. With an adopted temperature of $1-2\times 10^6$ K, similar to that of the galactic corona (Wolfire et al. 1995), the intergalactic pressure is less than ≈ 2000 K cm^{-3}, too low to confine the complexes.

We thus conclude that the molecular clouds are indeed gravitationally stable objects. The low observed main beam brightness temperature for all clouds indicates a low beam filling. If complex #1 is as cold as derived from our excitation study (Sect. 4.1) the observed mainbeam brightness temperature of only about 70 mK translates into a beam filling of 1/100. This implies that the large complex will probably break up into several smaller clouds when observed at higher angular resolution. Because the complex is extended the arguments hold for all of the

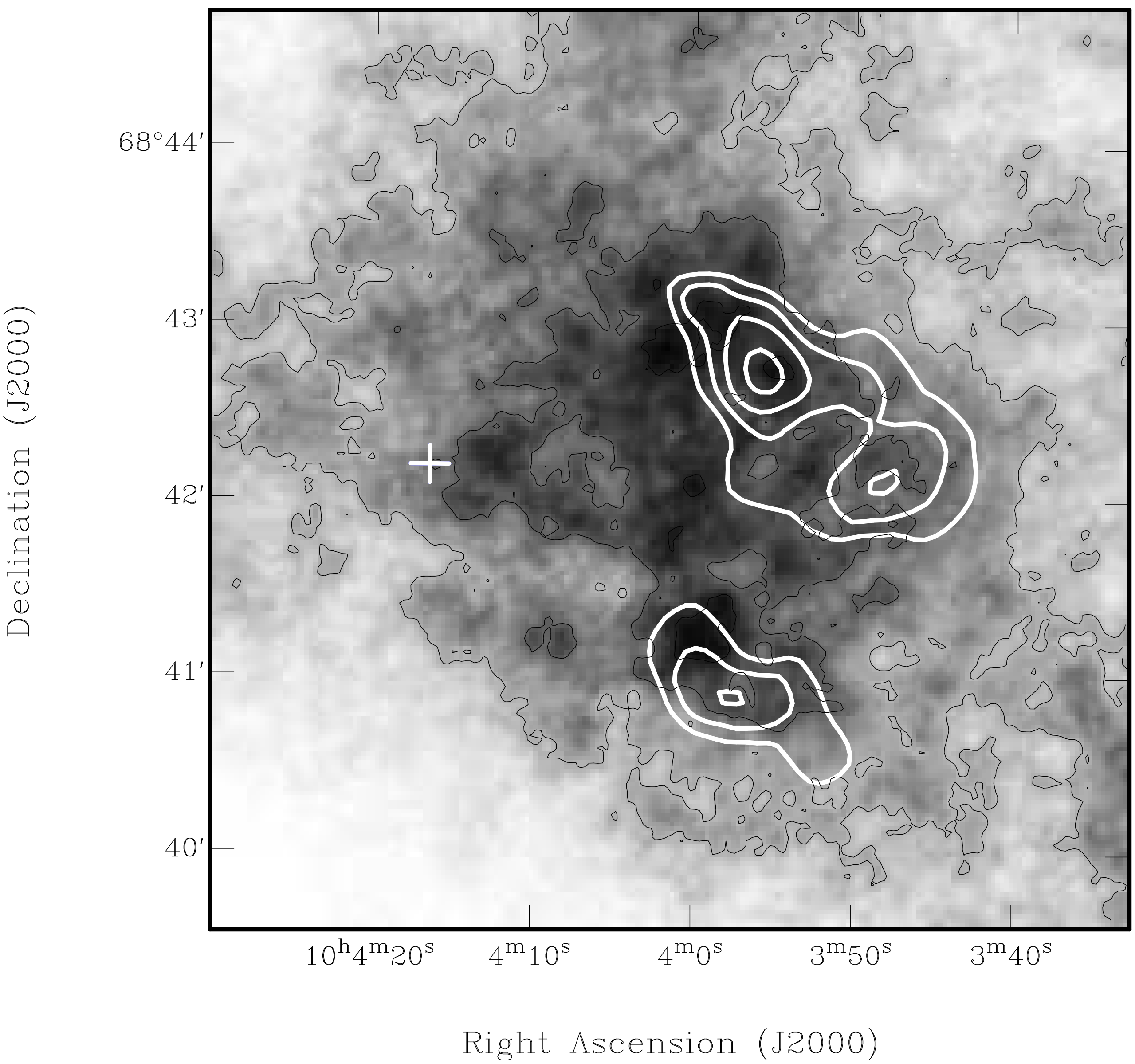

Fig. 6. Overlay of CO ($J = 1 \rightarrow 0$) contours on an integrated HI map (grey scale). Thick white (CO) contours are every 0.14 K km s^{-1} starting at 0.28 K km s^{-1}. Thin black contours represent HI column densities of 1×, 1.5×, and 2×10^{21} cm^{-2}. The + marks the position of complex #3. Note that the area has not fully been searched for CO, s. Fig. 1 for the sampling.

observed positions. This implies that the single clouds are spread over the area with an equivalent radius of 700 pc, and are not confined to one single massive cloud. High angular resolution interferometric CO studies will allow to investigate this situation further.

6. Conclusions

Our new observations have revealed extensive molecular gas in the tidal arms near NGC 3077. The CO emission is much more extended than previously thought – the detected complexes range among the most extended complexes in the local universe. We have detected at least three independent complexes of molecular gas. The complexes are most probably gravitationally bound and have formed *in situ*. For the largest of the complexes our multi-transition CO study shows that the gas must be cold (≈10 K), thus massive star formation is not going on at a significant level. Whether or not the chain of blue stars (the 'Garland') found in this region (Karachentsev et al. 1985a, 1985b) is associated with the molecular complex is an open question which is currently under investigation by us.

The fact that CO is found in tidal arms implies that galaxy interactions can efficiently remove enriched material from a galaxy's body hence influencing it's chemical history. This also has important implications for the chemical enrichment of the intergalactic medium (IGM), especially at larger look–back times in the universe where galaxy interactions may have been more frequent.

Since the tidal arm with its newly discovered molecular complexes has all the ingredients to form stars in the future (i.e., atomic and molecular gas), our new observation confirm our previous speculation (Walter & Heithausen 1999) that we are witnessing the birth of a dwarf galaxy where star formation might start in the near future. We are therefore in the fortunate situation to witness a process which may have created a substantial number of today's dwarf galaxies in the past.

Acknowledgements. We thank Christian Henkel for critically reading the manuscript and Andrea Tarchi for help with part of the observations. FW acknowledges NSF grant AST 96–13717. The KOSMA 3 m telescope is operated by the University of Cologne, Germany, and supported by the DFG grant SFB 301, as well as special funding from the Land NRW, Germany. The observatory is administered by the Internationale Stiftung Hochalpine Forschungsstationen Jungfraujoch und Gornergrat, Bern, Switzerland.

References

Barnes J.E., Hernquist L., 1996, ApJ 471 115
Becker R., Schilke P., Henkel C., 1989, A&A 211, L19
Bi H.G., Arp H., Zimmermann H.U., 1994, A&A 282, 386
Blake G.A., Sutton E.C., Masson C.R., Phillips T.G., 1987, ApJ 315, 621
Braine J., Lisenfeld U., Duc P.A., Leon S., 2000, Nat 403, 867
Brouillet N., Henkel C., Baudry A., 1992, A&A 262, L5
Charmandaris V., Combes F., van der Hulst J.M., 2000, A&A 356, L1
Cohen R.S., Dame T.M., Garay G., et al., ApJL 331, L95
Combes F., Dupraz C., Casoli F., Pagani, L., 1988, A&A 203, L9
Dame T.M., Ungerechts H., Cohen R.S., et al., 1987, ApJ 322, 706
de Jong T., Chu S.I., Dalgarno A., 1975, ApJS 199, 69
Elmegreen B., G., Kaufman M., Thomasson M., 1993, ApJ 412, 90
Hunsberger S.D., Charlton J.C., Zaritsky D., 1996, ApJ 462, 50
Jijina J., Myers P.C., Adams F.C, 1999, ApJS 125, 161
Karachentsev I.D., Karachentseva V.E., Börngen F., 1985a, A&A 60, 213
Karachentsev I.D., Karachentseva V.E., Börngen F., 1985b, MNRAS 217, 731
Lada C.J., Margulis M., Sofue Y., Nakai N., Handa T., 1988, ApJ 328, 143
Mirabel I.F., Lutz D., Maza J., 1991, A&A 243, 367
Mirabel I.F., Dottori H., Lutz D., 1992, A&A 256, L19
Pak S., Jaffe D.T., van Dishoeck E.F., Johanson L.E.B., Booth R.S., 1998, ApJ 498, 735
Savage B.D., Bohlin R.C., Drake J.F., Budich W., 1977, ApJ 216, 291
Smith B.J., Struck C., Kenney J.D.P., Jogee S., 1999, AJ, 117, 1237
Solomon P.M., Rivolo A.R., Barrett J., Yahil A., 1987, ApJ 319, 730
van der Hulst J.M., 1979, A&A 75, 97
Walter F., Heithausen A., 1999, ApJ 519, L69
Wolfire M., G., McKee C.F., Hollenbach D., Tielens A.G.G.M., 1995, ApJ 453, 673
Young L.M., Lo K.Y., 1997, ApJ 476, 127
Yun M.S., Ho P.T.P, Brouillet N., Lo K.Y. 1993, in 'The Evolution of Galaxies and Their Environment', eds. D. Hollenbach, H. Thronson, J.M. Shull, p. 253
Yun M.S., Ho P.T.P., Lo K.Y. 1994, Nat 372, 530
Zwicky F., 1956, Ergebnisse der Exakten Naturwissenschaften, 29, 344